Dalton Transactions

ROYAL SOCIETY OF CHEMISTRY

PAPER

View Article Online
View Journal | View Issue

Cite this: *Dalton Trans.*, 2023, **52**, 4768

Phenylimido complexes of rhenium: fluorine substituents provide protection, reactivity, and solubility†

Guilhem Claude,[a] Erika Kulitzki,[a] Adelheid Hagenbach,[a] Maximilian Roca Jungfer,[a] Joshua S. Figueroa *[b] and Ulrich Abram *[a]

Received 11th February 2023,
Accepted 7th March 2023

DOI: 10.1039/d3dt00446e

rsc.li/dalton

Reactions of $[Re(NPhF)Cl_3(PPh_3)_2]$ ($\{NPhF\}^{2-}$ = *p*-fluorophenylimide) with a variety of alkyl and aryl isocyanides have been studied. Different reactivity patterns and products have been obtained depending on the steric and electronic properties of the individual ligands. This involves the formation of 1 : 1 and 1 : 2 exchange products of Re(V) with the general formulae *mer*-$[Re(NPhF)Cl_3(PPh_3)(isocyanide)]$ and *cis*- or *trans*-$[Re(NPhF)Cl_3(isocyanide)_2]$. The stability of the obtained products is correlated with the substitution pattern of the isocyanide ligands. The products have been studied by single-crystal X-ray diffraction and spectroscopic methods, including IR and multinuclear NMR spectroscopy as well as mass spectrometry. The use of partially fluorinated starting materials and ligands allows the modulation of the solubilities of the starting materials and the products as well as the monitoring of the reactions by means of ^{19}F NMR. The attachment of the CF_3 or F substituent on the isocyanides gives control over the steric bulk and the electronic properties of the ligands and, thus, their reactivity.

Introduction

Fluorine possesses a series of peculiar properties. Its very high electronegativity (3.98 on the Pauling scale), as well as the strong hyperconjugation resulting from a low lying σ*(C–F) combined with its small atomic radius, has been shown to have profound structural and electronic effects on both organic and inorganic compounds.[1,2] Fluorine can therefore be introduced in biologically active molecules to increase their bioavailability and/or efficacy, which led to a significant growth of the number of small, fluorine-containing molecules considered for pharmaceutical applications. It was estimated that already in 2012 fluorinated compounds made 40% of all phase III drug candidates.[3]

In diagnostic nuclear medicine, the radioactive isotope ^{18}F is a common tracer in positron-emission tomography (PET), *e.g.* by replacing a "cold" fluorine atom by ^{18}F in an established pharmacologically active compound.[4–6] A hitherto relatively little considered option is the use of fluorine-substituted ligand systems for the modulation of the pharmacokinetic properties of metal-containing radiotracers, *e.g.* of the matched-pair $^{99m}Tc/^{188}Re$.[6–8] For the development of corresponding compounds, however, some fundamental work is required to learn more about the influence, which can be expected by partially fluorinated ligands in terms of the solubility and lipophilicity of the products, but also with regard to possible electronic effects. Such studies are commonly performed with natural rhenium and the long-lived technetium isotope ^{99}Tc (weak β^- emitter with E_{max} = 0.3 MeV, $t_{1/2} = 2.1 \times 10^5$ years), which is available in macroscopic amounts and allows the use of conventional spectroscopic methods including ^{19}F NMR spectroscopy, which is indicative of convenient monitoring of reactions.

Some recent work in our group with nuclear medically relevant metals such as indium, technetium or rhenium demonstrated that the structure and reactivity of metal complexes can markedly be influenced by (partial) fluorination of the ligands.[2,9–12] The observed changes in properties were found to be dependent on both the number of fluorine atoms and their exact position. The addition of sometimes even a single fluorine atom on a ligand also led to new reactivity patterns for both rhenium and technetium complexes. Thus, the use of *p*-fluorophenyl isocyanide instead of unsubstituted phenyl isocyanide resulted in completely different substitution patterns of *fac*-tricarbonyl complexes of these metals.[10,11]

Isocyanides are interesting ligands for nuclear medical procedures with ^{99m}Tc and probably also for ^{188}Re. ^{99m}Tc-Sestamibi (Cardiolite), an octahedral technetium(I) complex

[a]*Freie Universität Berlin, Institute of Chemistry and Biochemistry, Fabeckstr. 34/36, 14195 Berlin, Germany. E-mail: ulrich.abram@fu-berlin.de*
[b]*University of California San Diego, La Jolla, Department of Chemistry and Biochemistry, California 92093, USA. E-mail: jsfig@ucsd.edu*

†Electronic supplementary information (ESI) available. CCDC 2236802–2236812. For ESI and crystallographic data in CIF or other electronic format see DOI: https://doi.org/10.1039/d3dt00446e

with six methoxy-substituted isocyanides, is one of the most used diagnostic radiopharmaceuticals worldwide.[12–15] Isocyanide complexes with high-valent rhenium and technetium centers are rare and only a few examples of oxidorhenium(v) complexes are known,[16–18] while the corresponding $\{TcO\}^{3+}$ core is prone to reduction by isocyanides and no such compounds could be isolated until now.

More stable against reduction is the isoelectronic phenylimido core and some technetium isocyanide complexes with a central $\{Tc(NPh)\}^{3+}$ unit could be isolated.[19,20] A number of interesting reactivity features have been observed during this study, which makes it interesting to have a look at the related chemistry of rhenium.

The phenylimido complex $[Re(NPh)Cl_3(PPh_3)_2]$ is isoelectronic to the oxidorhenium(v) compound $[ReOCl_3(PPh_3)_2]$, which is frequently used as a common precursor for ligand exchange procedures.[21] A similar use of the phenylimido compound as the starting material may give access to a wide variety of phenylimido complexes. Unfortunately, the rhenium compound is significantly less soluble than its technetium analog. Thus, predominately reactions with strong chelators or with robust ligands,[22–45] which resist harsh reaction conditions, give pure products in good yields. The corresponding bromido complex $[Re(NPh)Br_3(PPh_3)_2]$ is slightly more soluble and is, thus, occasionally used as a better suitable starting material.[37,40,44,45] Alternatively, substitutions on the arylimido ligand with the carboxylic, hydroxylic or amine group provide an enhanced solubility.[46–50] Such residues, however, sometimes undergo undesired reactions with co-ligands and/or solvents (*e.g.* esterification, formation of Schiff bases, *etc.*), which frequently causes undesired side-reactions and/or lower yields. A modulation of the solubility of the phenylimido starting material without significant interference with the chemical behaviour of other ligands has recently been demonstrated with the use of *p*-fluoro-substituted phenylimido ligands in $[M(NPhF)Cl_3(PPh_3)_2]$ complexes, M = Tc or Re (**1**).[51,52]

In the present report, we present a series of (fluorinated) phenylimidorhenium(v) complexes with a variety of different alkyl and aryl isocyanides (Fig. 1).

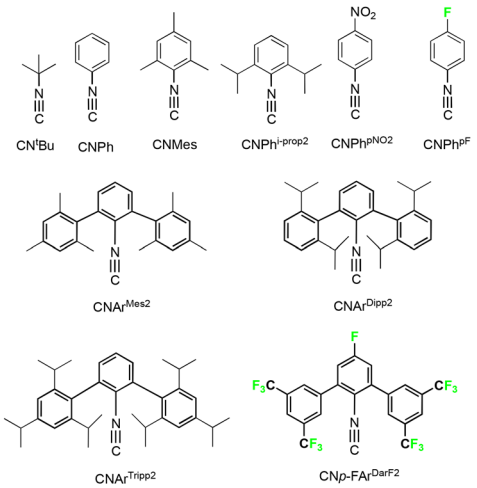

Fig. 1 Isocyanides used throughout this paper.

Results and discussion

The attachment of a fluorine atom to the phenylimido ligand of $[Re(NPh)Cl_3(PPh_3)_2]$ increases the room temperature-solubility by a factor of 5 in both dichloromethane and acetonitrile. This allows for milder reaction conditions and lower temperatures, which is particularly beneficial for sensitive isocyanides such as CNPh, CNMes or CNPh^{pNO2} of the present study. These ligands as well as other common isocyanides such as CN^{t}Bu or CNPh$^{i\text{-prop2}}$ react with $[Re(NPhF)Cl_3(PPh_3)_2]$ (**1**) with the formation of mono-substituted complexes of the composition $[Re(NPhF)Cl_3(PPh_3)(CNR)]$ (Scheme 1). The reactions have first been performed with an excess of ligands and for the more stable ligands (CN^{t}Bu and CNPh$^{i\text{-prop2}}$) also prolonged reactions at higher temperatures have been tested. In both cases, exclusively 1 : 1 ligand exchange products could be isolated. The gradual (not metal-driven) decomposition of the isocyanides, however, caused significant problems during the isolation of pure products in these cases. For this reason, relatively short reaction times and only a slight excess of the ligands have been used in optimized procedures. Even so, only a small amount of pure products could be obtained from some of the sensitive isocyanides.

The formation of 1 : 1 complexes with common isocyanides has also been observed for reactions of $[Tc(NPh)Cl_3(PPh_3)_2]$,[20] and for reactions of robust isocyanides with the corresponding phenyl- or tolyl- or xylylimido complexes.[46,53–55] These findings are not necessarily trivial since the ligand exchange behaviour of isocyanides has been found to be strongly dependent on steric and electronic factors. In particular, electronic effects due to electron withdrawing or electron donating substituents on (phenyl) isocyanides have been underestimated in the coordination chemistry of these compounds. Systematic studies about this point are rare, which is attributed to the preferred use of commercially available and stable ligands such as *e.g. tert*-butyl or cyclohexyl isocyanide in many papers about the related chemistry. Approximately 40 percent of all studies with isocyanides are done with these two representatives. A nice overview of this point is given in ref. 56. This, finally, resulted in a (not fully justified) generalization of their chemical behaviour for all isocyanides. After the exploration of the coordination chemistry of the bulky (but also electronically diverse) *m*-terphenyl isocyanides,[57–69] it became evident that isocyanides are more than bulky surrogates of carbonyl ligands. This also includes studies on group 7 elements, which have been stabilized in oxidation states ranging from '−1' to '+5'.[10,11,20–22,70,71] A DFT-based sum parameter describing the electronic potential on the accessible VdW surface of the isocyanide carbon atom has recently been derived for a number of isocyanides.[10] The so-called SADAP (surface-averaged donor acceptor potential) parameter is a combined descriptor of the steric and electrostatic properties of the potential ligand.

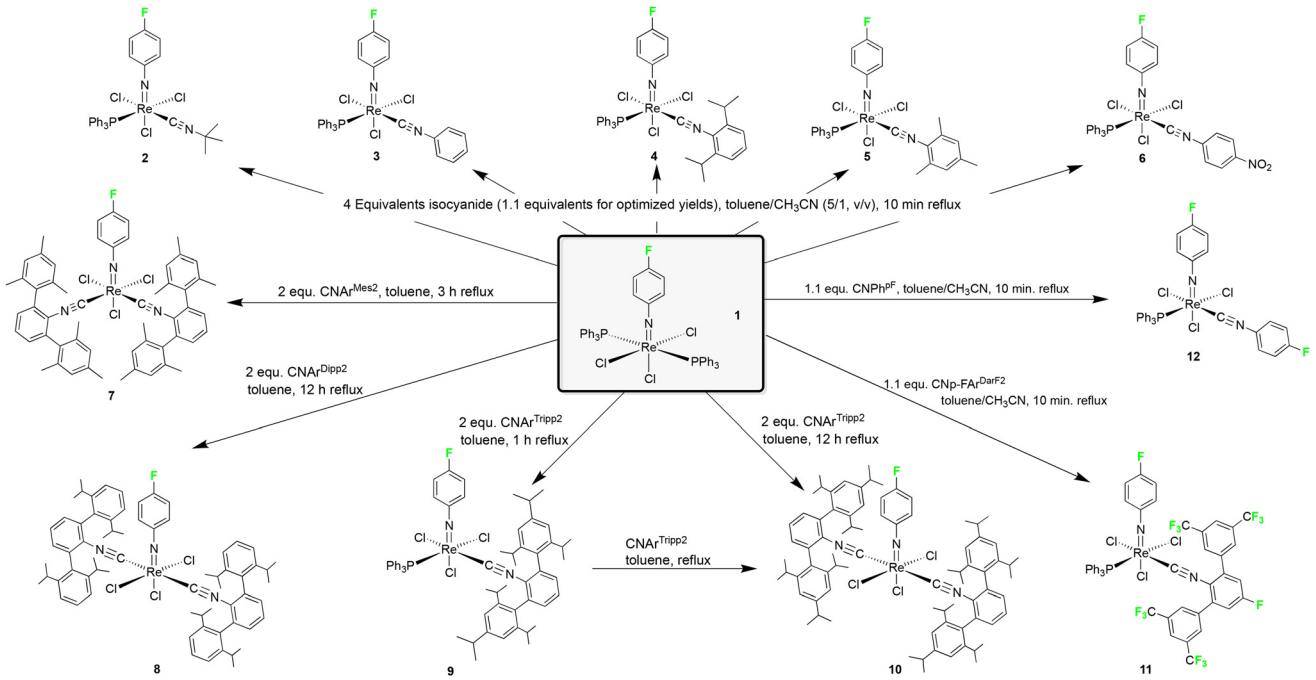

Scheme 1 Reaction of $[Re(NPhF)Cl_3(PPh_3)_2]$ with various isocyanides.

Table 2 contains selected SADAP parameters for the isocyanides of the present study. Details of the calculations and the derived parameter comprising a large number of isocyanides are outlined in ref. 10. Such parameters nicely describe the reactivity of a number of carbonyltechnetium(I) complexes, where ligands with progressively electron-deficient properties readily replace carbonyl ligands, while those with a large negative potential at the carbon atoms are σ-donors with predominantly negligible back-donation properties.[10] Similar considerations have also been done for phenylimidotechnetium(V) compounds, d^2 systems, where π-acceptor behaviour should be negligible.[20]

The formation of 1 : 1 complexes during reactions of $[Re(NPhF)Cl_3(PPh_3)_2]$ with the relatively electron-deficient isocyanides as shown in Fig. 1 is in line with such considerations. The $\nu_{C\equiv N}$ IR stretches of the complexes appear between 2158 and 2192 cm^{-1}. These values are significantly higher (between 39 and 72 cm^{-1}, for individual values see the Experimental section) than those in the spectra of uncoordinated isocyanides, which means that there is no sign for π-backdonation into anti-bonding orbitals of the ligands in the d^2 complexes under study.

Ellipsoid plots of the molecular structures of the $[Re(NPhF)Cl_3(PPh_3)(CNR)]$ complexes (R = ^{t}Bu, Ph, Ph$^{i\text{-prop2}}$, Mes, Ph^{pNO2}) are depicted in Fig. 1. Selected bond lengths and angles are summarized in Table 1. The Re–N bonds are clearly in the range of double bonds and the slightly bent phenylimido units (Re–N–C angles between 164 and 173°) are a common feature of such compounds.[22–45] The replacement of one of the PPh_3 ligands of $[Re(NPhF)Cl_3(PPh_3)_2]$ goes along with a rearrangement of the coordination sphere of rhenium. The incoming isocyanides are found in *cis* position to phosphine in all 1 : 1 complexes.

Two isocyanide ligands could be bonded to a $\{ReNPhF\}^{3+}$ unit, when more electron-rich isocyanides such as CNAr^{Mes2}, CNAr^{Dipp2} or CNAr^{Tripp2} were used. The steric bulk of the individual ligands, however, has an influence on the isomers formed. The reaction of the less bulky CNAr^{Mes2} gives the 1 : 2

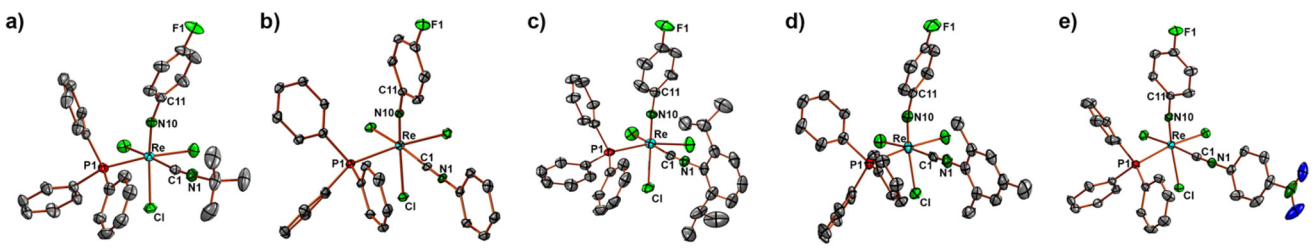

Fig. 2 Molecular structures of (a) $[Re(NPhF)Cl_3(PPh_3)(CN^tBu)]$ (**2**), (b) $[Re(NPhF)Cl_3(PPh_3)(CNPh)]$ (**3**), (c) $[Re(NPhF)Cl_3(PPh_3)(CNPh^{i\text{-prop2}})]$ (**4**), (d) $[Re(NPhF)Cl_3(PPh_3)(CNMes)]$ (**5**) and (e) $[Re(NPhF)Cl_3(PPh_3)(CNPh^{pNO2})]$ (**6**).

Table 1 Selected bond lengths and angles of $[Re(NPhF)Cl_3(PPh_3)(CNR)]$ complexes

	2[a]	3	4	5	6	11	12
Re–N10	1.715(3), 1.715(3)	1.731(3)	1.722(3)	1.712(3)	1.711(3)	1.721(3)	1.705(4)
N10–C11	1.391(4), 1.382(4)	1.377(4)	1.385(4)	1.399(5)	1.390(5)	1.380(4)	1.395(7)
Re–P1	2.4593(9), 2.4473(9)	2.4539(9)	2.4476(9)	2.463(1)	2.454(1)	2.4494(8)	2.470(2)
Re–C1	2.020(4), 2.045(4)	2.028(4)	2.023(3)	2.030(4)	2.020(5)	2.022(3)	2.024(6)
C1–N1	1.151(5), 1.146(5)	1.165(5)	1.147(4)	1.151(6)	1.162(6)	1.151(4)	1.156(7)
Re–N10–C11	164.4(3), 166.7(2)	168.7(3)	172.1(2)	166.0(3)	171.2(3)	170.4(2)	172.9(4)
Re–C1–N1	172.9(3), 173.8(8)	177.7(3)	170.6(3)	176.9(3)	176.6(4)	174.6(3)	176.9(4)
N10–Re–P1	93.1(1), 91.42(9)	89.99(9)	94.15(9)	92.0(1)	94.2(1)	91.96(8)	94.2(2)
N10–Re–C1	86.0(1), 88.1(1)	87.7(1)	88.1(1)	85.7(1)	89.4(2)	88.5(1)	91.8(2)

[a] Values of two crystallographically independent species.

complex *fac*-$[Re(NPhF)Cl_3(CNAr^{Mes2})_2]$ (**7**) with the two isocyanide ligands in *cis* position to each other, while the corresponding *trans* complexes are formed by the sterically more encumbered ligands $CNAr^{Dipp2}$ and $CNAr^{Tripp2}$ (Scheme 1). The formation of *cis* complexes with $CNAr^{Mes2}$ is a common feature of this ligand and has also been observed for oxido and nitrido complexes of rhenium and technetium.[18,19] There are even some rare cases where three $CNAr^{Mes2}$ ligands are accommodated in octahedral complexes of cobalt,[72] molybdenum,[58,73] and manganese.[62] Such flexibility regarding the number of ligands and their coordination positions, however, is also the source of the appearance of a fluxional behaviour in solution, which could be detected preferably by ^{19}F NMR, with subsequent problems for the isolation of satisfactory amounts of the individual species in pure form. This is mainly due to the almost identical solubility of the formed species and also applies to the phenylimido compounds under study with the consequence that only a relatively small amount of complex **7** could be isolated in crystalline form. Although the isolated blue needles of **7** were identical as has been tested by X-ray diffraction on several species, they quickly isomerize in solution and again several ^{19}F NMR signals are detected. This behaviour is unlike that of the complexes with the more bulky $CNAr^{Dipp2}$ or $CNAr^{Tripp2}$ ligands, which form inert *mer*-$[Re(NPhF)Cl_3(isocyanide)_2]$ complexes that contain the isocyanides necessarily in *trans* position to each other.

Ellipsoid plots of the molecular structures of complex *fac*-$[Re(NPh)Cl_3(CNAr^{Mes2})_2]$ (**7**) and *mer*-$[Re(NPhF)Cl_3(CNAr^{Dipp2})_2]$ (**8**) are shown in Fig. 3. All common features of the central $\{Re(NPhF)\}^{3+}$ unit discussed above for compounds **2–6** (Re–N double bond, slightly bent Re–N10–C11 axis) also apply for the bis complexes **7** and **8**. The rhenium-carbon bonds in the *cis* isomer **7** (2.034–2.044 Å) are slightly shorter than in the *trans* isomer **8** (2.055–2.076 Å). This comes not unexpected with regard to the sterically favoured *trans* compound. Similar effects have been observed previously for the *cis* and *trans* isomers of $[Re(CO)_3Br(CNAr^{Dipp2})_2]$, where the Re–C (isocyanide) bonds are elongated by approximately 0.02 Å in *trans* position to carbonyl ligands,[70] for which, however, mainly electronic effects shall be responsible.

The exchange of the PPh_3 ligands occurs stepwise and can nicely be monitored by ^{19}F NMR. Fig. 4 shows ^{19}F NMR spectra

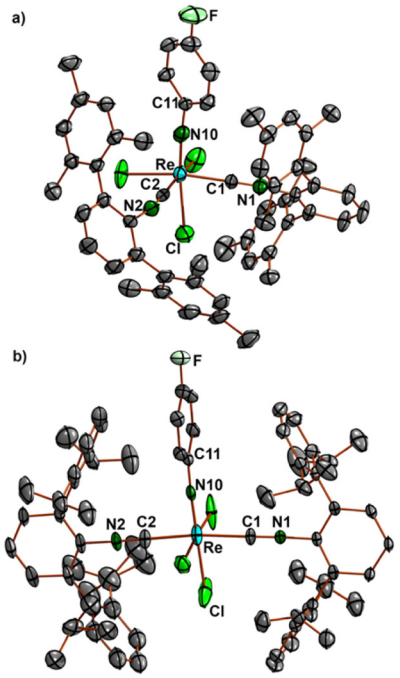

Fig. 3 Molecular structures of (a) *fac*-$[Re(NPh)Cl_3(CNAr^{Mes2})_2]$ (**7**) and (b) *mer*-$[Re(NPhF)Cl_3(CNAr^{Dipp2})_2]$ (**8**) (selected bond lengths and angles of **7**: Re–N10 1.724(3), Re–C1 2.043(4), Re–C2 2.034(4) Å, Re–N10–C11 173.0(3), Re–C1–N1 176.6(3), and Re–C2–N2 174.2(4)°; selected bond lengths and angles of **8**: Re–N10 1.728(7) and 1.722(6), Re–C1 2.076(6) and 2.066(6), Re–C2 2.055(7) and 2.055(7) Å, Re–N10–C11 177.4(5) and 171.5(5), Re–C1–N1 179.1(7) and 178.2(6), and Re–C2–N2 176.6(7) and 178.3(6)°. The values of compound **8** refer to two independent molecular species.

recorded for a corresponding reaction of $[Re(NPhF)Cl_3(PPh_3)_2]$ (**1**) with $CNAr^{Dipp2}$ in toluene. The formation of two transient compounds can readily be detected by their ^{19}F NMR signals in addition to the signals of the (not yet consumed) starting material **1** in the initial phase (first hour) of the reaction. Upon subsequent heating, the intensities of these signals and of compound **1** decrease in favour of the formation of the final product of the reaction *mer*-$[Re(NPhF)Cl_3(CNAr^{Dipp2})_2]$ (**8**). The tentative assignment of the transient signals **A** and **B** is possible in two ways: (1) to a mixture of *cis*- and *trans*-[Re(NPhF)

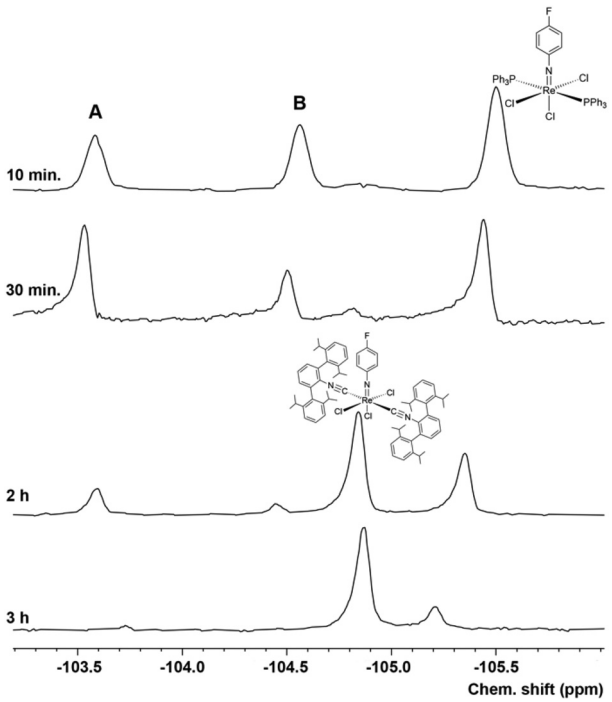

Fig. 4 ^{19}F NMR monitoring of a reaction mixture of [Re(NPhF)$Cl_3(PPh_3)_2$] and two equivalents of $CNAr^{Dipp2}$ in boiling toluene. Note the narrow chemical shift range depicted and that the chemical shifts slightly differ from the values given in the Experimental part due to solvent effects.

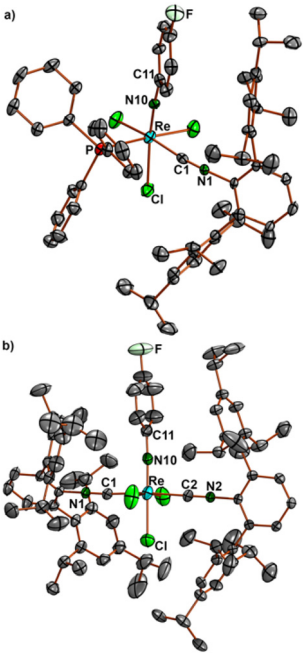

Fig. 5 Molecular structures of (a) *fac*-[Re(NPh)$Cl_3(PPh_3)(CNAr^{Tripp2})$] (**9**) and (b) *mer*-[Re(NPhF)$Cl_3(CNAr^{Tripp2})_2$] (**10**). Selected bond lengths and angles of **9**: Re–N10 1.711(4), Re–P 2.460(2), Re–C1 2.027(5), C1–N1 1.167(5) Å; Re–N10–C11 168.7(3), and Re–C1–N1 170.4(4)°. Selected bond lengths and angles of **10**: Re–N10 1.698(6) and 1.711(5), Re–C1 2.093(6) and 2.090(6), Re–C2 2.084(6) and 2.076(6), C1–N1 1.135(7) and 1.139(7), C2–N2 1.135(7) and 1.148(7) Å; Re–N10–C11 177.1(5) and 178.7(5), Re–C1–N1 175.3(6) and 178.2(6), and Re–C2–N2 175.4(5) and 179.5(7)°. The values of compound **10** refer to two independent molecular species.

$Cl_3(PPh_3)(CNAr^{Dipp2})$] or (2) to a mixture of *cis*-[Re(NPhF)$Cl_3(PPh_3)(CNAr^{Dipp2})$] and [Re(NPhF)$Cl_3(PPh_3)(CNAr^{Dipp2})_2$]. Evidence for the latter, seven-coordinate species is given with the detection of an intense peak at m/z = 1349.600 (simulation: 1349.309) in the ESI + mass spectrum of the reaction mixture after 10 min. Up to now, we could not isolate these two or at least one of these complexes in crystalline form for an unambiguous proof of one of these assumptions. This, however, was possible for the corresponding reaction with $CNAr^{Tripp2}$.

The ^{19}F NMR monitoring of the reaction of **1** with $CNAr^{Tripp2}$ (see the ESI, Fig. S57†) shows that essentially only one major transient compound is formed. The concentration of this compound reaches a maximum after approximately 90 min and when the reaction is stopped at this point, a small amount of this intermediate can be separated from the bulk of the starting material **1** and crystallized. An X-ray diffraction study on these single crystals confirms the formation of *fac*-[Re(NPhF)$Cl_3(PPh_3)(CNAr^{Tripp2})$] (**9**) as the (isolated) intermediate of this reaction. Prolonged heating of the reaction mixtures gives the bis complex [Re(NPhF)$Cl_3(CNAr^{Tripp2})_2$] (**10**) similar to the reaction with $CNAr^{Dipp2}$. The molecular structures of compounds **9** and **10** are depicted in Fig. 5. Bond lengths and angles in the products with the extremely sterically encumbered $CNAr^{Tripp2}$ ligand are similar to those observed in the other 1 : 1 complexes or in the analogous bis complex with $CNAr^{Dipp2}$ discussed above. Also in compound **10**, the Re–C bonds are slightly longer than in the complexes of the composition [Re(NPhF)$Cl_3(PPh_3)(CNR)$], where the isocyanides are in *trans* positions to chlorido ligands.

$CNAr^{Dipp2}$ and $CNAr^{Tripp2}$ are structurally distinguished by the presence of additional isopropyl substituents at the peripheral phenyl rings. At first glance this seems to be a minor difference, especially since this substitution is in the 4-position and, thus, relatively far away from the coordinating carbon atom. This means, that a similar electronic potential should be expected for both ligands, while $CNAr^{Tripp2}$ should be slightly more sterically hindered, which is finally also reflected by the SADAP parameters in Table 2 and the formation of 1 : 2 complexes of the present study. Nevertheless, there is a striking difference between these two isocyanides

Table 2 Selected SADAP parameters of the isocyanides of the present study. Values are taken from ref. 10 and 20

Isocyanide	SADAP
$CNAr^{Tripp2}$	−3.33
$CNAr^{Dipp2}$	−3.28
$CNPh^{i\text{-}prop2}$, CNMes, CN^tBu	−2.38, −2.26, −2.15
CNPh, $CNPh^{pNO2}$	−1.64, −0.95
$CNPh^{pF}$	−1.25
$CNp\text{-}FAr^{D^3rF2}$	+2.73

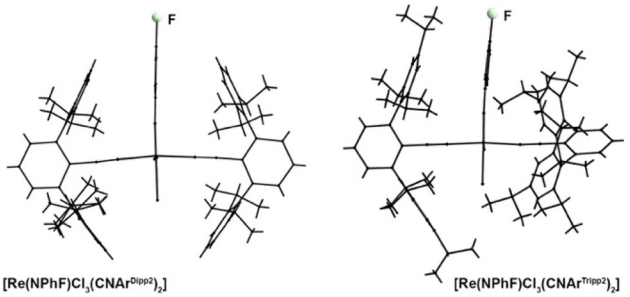

Fig. 6 Wire-frame presentation of the structures of *mer*-[Re(NPh)Cl_3($CNAr^{Dipp2}$)$_2$] (**8**) and *mer*-[Re(NPhF)Cl_3($CNAr^{Tripp2}$)$_2$] (**10**) along the planes formed by their phenylimido ligands.

regarding their steric bulk. This can nicely be seen in Fig. 6, where the solid state structures of [Re(NPhF)Cl_3($CNAr^{Dipp2}$)$_2$] (**8**) and [Re(NPhF)Cl_3($CNAr^{Tripp2}$)$_2$] (**10**) are shown along the planes formed by their phenylimido ligands. The central phenyl rings of the two $CNAr^{Dipp2}$ ligands are almost perfectly co-planar (twisting angle: 7.1(6)°) in a perpendicular arrangement to the phenylimido ring. The larger bulk of $CNAr^{Tripp2}$ results in a torsion of 52.3(2)° of the isocyanide ligand around its coordination axis. This is a direct effect of the 'outer-sphere' substitution on this ligand and may underline the influence of such relatively small modifications in the ligand design on structural factors, but also on the reactivity of the respective metal ion. It shall be noted that the proton NMR resonances of $CNAr^{Tripp2}$ appear as one set of signals suggesting that a rotation is possible in solution.

The steric effects discussed above shall always be regarded together with potential electronic effects due to the introduced residues and the electronic configuration of the metal ion. An example of the complex interplay of such influences shall be discussed with the use of the fluorinated isocyanides CNp-FAr^{DarF2} and $CNPh^{pF}$.

The steric bulk of CNp-FAr^{DarF2} due to the CF_3 residues in *meta* positions of the terphenyl rings takes mainly effect in the outer sphere of the complex similar to $CNAr^{Tripp2}$, but the fluorinated ligand is more flexible in terms of a spheric arrangement around the metal ions. Thus, it allows the coordination of up to four of the ligands around a metal ion. This has been demonstrated recently for carbonyl complexes of manganese, technetium and rhenium, where compounds of the compositions $[M^{-I}(CO)(CNp\text{-}FAr^{DarF2})_4]^-$ (M = Tc, Re), $[M^0(CO)(CNp\text{-}FAr^{DarF2})_4]$ (M = Tc, Re) and $[M^I(CO)(CNp\text{-}FAr^{DarF2})_4]$ (M = Tc, Re) have been isolated in crystalline form.[71,74] The replacement of carbonyl ligands from tricarbonylrhenium(I) or technetium(I) centers is not common and can be attributed to the special electronic situation on the donor carbon atom due to the strong electron withdrawing capacity of the fluorine atom at the central phenyl ring of CNp-FAr^{DarF2}.

For isocyanides, it is reasonable to assume that electron-deficient regions on the surface of the coordinating carbon atom would enable improved π-back-donation, while electron-rich regions on the surface of the same carbon atom are responsible for a better σ-donation. Steric restraints on the donor carbon atom can be partially included in such an approach by averaging the obtained potential energies over the accessible surface of the potential donor atoms.

Thus, sterically demanding isocyanides such as $CNAr^{Dipp2}$ or $CNAr^{Tripp2}$ show less overall accessible surface area, while the less encumbered isocyanides have a larger overall accessible carbon surface. A more comprehensive discussion of this approach is shown in ref. 10. In the sterically encumbered, but fluorine-substituted CNp-FAr^{DarF2} ligand the steric effects are overruled by the electron withdrawing capacity of fluorine, which make this ligand a powerful π-acceptor when it reacts with electron rich metal ions such as rhenium(I) or technetium(I) and explains the reactivity with the corresponding carbonyl compounds.[10,11,20] In the electron-deficient rhenium(V) complexes of the present study, however, π-back-donation plays practically no role, which is supported by the blue-shift of the IR $\nu_{C\equiv N}$ frequencies. Consequently, the reactivity of CNp-FAr^{DarF2} in such cases is identical with those isocyanides with predominantly σ-donor properties and [Re(NPhF)Cl_3(PPh_3)(CNp-FAr^{DarF2})] (**11**) is formed as the sole product in a reaction with **1**. The corresponding reactivity is well reflected by the SADAP parameters in Table 2.

A similar behavior is observed for $CNPh^{pF}$, where the fluorine substitution at the central ring is retained, but the steric bulk due to the peripheral residuals is removed. Indeed, it behaves with electron-rich metal ions as a powerful π-acceptor, as has been demonstrated by the complete replacement of carbonyl and halido ligands in $[Tc_2(CO)_6Cl_3]^{2-}$ and the formation of a $[Tc(CNPhpF)_6]^+$ cation.[20] Expectedly, this is not observed for the d^2 complexes of the present study and the 1 : 1 complex [Re(NPhF)Cl_3(PPh_3)($CNPh^{pF}$)] (**12**) was isolated from a corresponding reaction with compound **1**.

The structures of compounds **11** and **12** are shown in Fig. 7. All main structural features are close to those of the other 1 : 1 complexes presented in Fig. 2 and Table 1 and shall not be discussed here in detail.

Experimental

General considerations

Unless otherwise stated, reagent-grade starting materials were purchased from commercial sources and either used as received or purified by standard procedures. Solvents were dried according to standard procedures. The reactions have been performed in air unless otherwise stated. [Re(NPh^{pF})Cl_3(PPh_3)] (**1**) as well as $CNAr^{Dipp2}$, $CNAr^{Tripp2}$, CNp-FAr^{DarF2}, $CNPh^{pF}$, and $CNPh^{i\text{-}prop2}$ were prepared according to literature procedures.[10,51,56,58,59]

Physical measurements

NMR spectra were recorded with JEOL 400 MHz ECS or ECZ or JEOL ECZ 600 or Bruker AV700 multinuclear spectrometers. IR spectra were recorded with an ATR spectrometer (Nicolet iS10, Thermo Scientific). Intensities are classified as vs = very

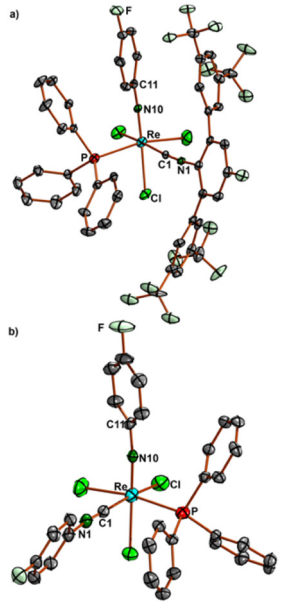

Fig. 7 Molecular structures of a) *fac*-[Re(NPh)Cl_3(PPh_3)($CNAr^{DarF2}$)$_2$] (**11**) and b) *mer*-[Re(NPhF)Cl_3(PPh_3)($CNPh^{pF}$)$_2$] (**12**). Selected bond lengths and angles for **11**: Re–N10 1.721(43), Re–P 2.4494(9), Re–C1 2.022(3), C1–N1 1.151(4) Å; Re–N10–C11 170.4(2), and Re–C1–N1 174.6(43)°; selected bond lengths and angles of **12**: Re–N10 1.705(4), Re–P 2.470 (2), Re–C1 2.024(6), C1–N1 1.156(7) Å; Re–N10–C11 172.9(4), and Re–C1–N1 176.9(5)°.

strong, s = strong, m = medium, w = weak, vw = very weak, and sh = shoulder. Electrospray ionization mass spectrometry (ESI MS) was carried out with the ESI MSD time-of-flight (TOF) unit of an Agilent 6210 TOF liquid chromatography/mass spectrometry system. Elemental analyses of carefully dried samples of the bulk were performed using a Vario MICRO cube CHNS elemental analyser.

X-ray crystallography

The intensities for X-ray determinations were collected on STOE IPDS II or Bruker D8 Venture instruments with Mo Kα radiation. The space groups were determined by the detection of systematic absences. Absorption corrections were carried out by multi scan or integration methods.[75,76] Structure solution and refinement were performed with the SHELX program package using OLEX 2.[77–79] Hydrogen atoms were derived from the final Fourier maps and refined or placed at calculated positions and treated with the 'riding model' option of SHELXL. The representation of molecular structures was done using the program DIAMOND 4.2.2.[80]

Additional information on the structure determinations is presented in the ESI† and has been deposited with the Cambridge Crystallographic Data Centre.

Synthesis

[Re(NPhF)Cl_3(PPh_3)(CNR)] complexes. [Re(NPhF)Cl_3(PPh_3)$_2$] (**1**) (92 mg, 0.1 mmol) was suspended in a 5 : 1 toluene/acetonitrile mixture (6 mL) and the corresponding isocyanide (0.11 mmol) was added. The mixture was heated under reflux for 10 min in a pre-heated oil bath. The starting material dissolved and the solution turned blue or green. Volatiles were removed under reduced pressure and the residue was resuspended in diethyl ether (5 mL) and filtered. The obtained solid was washed with diethyl ether (3 × 5 mL) and dried under reduced pressure.

***fac*-[Re(NPhF)Cl_3(PPh_3)(CN^tBu)] (2).** Recrystallization from CH_2Cl_2/diethyl ether. Light blue plates. Yield: 36 mg, 48%. Elemental analysis: calc.: C: 46.6, H: 3.8, N: 3.7%. Found: C: 46.7, H: 3.8, N: 3.8%. IR (cm^{-1}): 2192 (vs, $\nu_{C\equiv N}$), 1584 (vs). ^{1}H NMR (CD_2Cl_2, ppm): δ = 7.75 (m_c, 6H), 7.42 (m_c, 9H), 7.02 (m_c, 2H,), 6.82 (t, J = 8.0 Hz, 2H), 1.43 (s, 9H). ^{19}F NMR (CD_2Cl_2, ppm): δ = −101.9 (m_c). $^{13}C\{^1H\}$ NMR (CD_2Cl_2, ppm): δ = 162.83 (d, $^1J(^{13}C–^{19}F)$ = 260 Hz), 151.32, 135.01 (d, $J(^{13}C–^{31}P)$ = 8 Hz), 133.73 (d, $^1J(^{13}C–^{31}P)$ = 53 Hz), 131.74, 128.90 (d, $J(^{13}C–^{31}P)$ = 10 Hz), 127.09 (d, $^3J(^{13}C–^{19}F)$ = 10 Hz), 117.55 (d, $^2J(^{13}C–^{19}F)$ = 25 Hz), 60.30, 31.24. ESI + MS: m/z = 628.0141 [M − CN^tBu − Cl]$^+$ (calc.: 628.0158), 711.0855 [M − Cl]$^+$ (calc.: 711.0894), 769.0463 [M + Na]$^+$ (calc.: 769.0494), 1517.069 [2M + Na]$^+$ (calc.: 1517.0999).

***fac*-[Re(NPhF)Cl_3(PPh_3)(CNPh)] (3).** Single crystals were obtained directly from the reaction mixture at 5 °C. Green, sensitive blocks. Only a small amount of the compound could be isolated in this way, since it quickly decomposes in solution even at room temperature precluding the measurement of spectra of appropriate quality. Already the uncoordinated CNPh is significantly more unstable than other isocyanides in this study. IR (cm^{-1}): 2171 (vs, $\nu_{C\equiv N}$). ESI + MS: m/z = 731.0669 [M − Cl]$^+$ (calc.: 731.0581), 789.0183 [M + Na]$^+$ (calc.: 789.01622), 804.9920 [M + K]$^+$ (calc.: 804.9901), 1557.0502 [2M + Na]$^+$ (calc.: 1557.0417).

***fac*-[Re(NPhF)Cl_3(PPh_3)($CNPh^{i\text{-}prop2}$)] (4).** Recrystallization from CH_2Cl_2. Blue crystals. Yield: 44 mg, 52%. Elemental analysis: calc.: C: 52.2, H: 4.3, N: 3.3%. Found: C: 52.2, H: 4.3, N: 3.5%. IR (cm^{-1}): 2168 (vs, $\nu_{N\equiv C}$). ^{1}H NMR (CD_2Cl_2, ppm): δ = 7.81 (m_c, 6H), 7.39 (m_c, 3H), 7.34 (m_c, 6H), 7.26–7.19 (m, 3H), 7.03(m_c, 2H), 6.86 (m_c, 2H), 2.71 (h, $^3J(^1H, ^1H)$ = 7 Hz, 2H), 1.00 (d, $^3J(^1H, ^1H)$ = 7 Hz, 6H), 0.92 (d, $^3J(^1H, ^1H)$ = 7 Hz, 6H). ^{19}F NMR (CD_2Cl_2, ppm): δ = −101.9 (m_c). $^{13}C\{^1H\}$ NMR (CD_2Cl_2, ppm): δ = 162.86 (d, $^1J(^{13}C,^{19}F)$ = 260 Hz), 151.45 (t, $^1J(^{13}C,^{14}N)$ = 3 Hz), 145.48, 135.02 (d, $J(^{13}C,^{31}P)$ = 9 Hz), 133.45 (d, $^1J(^{13}C,^{31}P)$ = 45 Hz), 131.87 (d, $J(^{13}C,^{31}P)$ = 2 Hz), 131.30, 129.01 (d, $J(^{13}C,^{31}P)$ = 11 Hz), 126.93 (d, $^3J(^{13}C,^{19}F)$ = 10 Hz), 123.41, 117.58 (d, $^2J(^{13}C,^{19}F)$ = 25 Hz), 29.74, 23.51, 22.86. ESI + MS: m/z = 873.109 [M + Na]$^+$ (calc.: 873.112), 889.084 [M + K]$^+$ (calc.: 889.086), 1725.233 [2M + Na]$^+$ (calc.: 1723.234), 1739.209 [2M + K]$^+$ (calc.: 1739.208).

***fac*-[Re(NPhF)Cl_3(PPh_3)(CNMes)] (5).** A few single crystals were obtained upon cooling the reaction mixture. Green-blue, sensitive blocks. Only a small amount of the compound could be isolated in this way, since it quickly decomposes in solution even at room temperature precluding the measurement of spectra of appropriate quality. IR (cm^{-1}): 2173 (vs, $\nu_{N\equiv C}$). ^{1}H NMR (CD_2Cl_2, ppm): δ = 7.78 (m_c, 6H), 7.34 (m_c, 9H), 7.04 (m_c, 2H), 6.92 (s, 2H), 6.83 (dd, $^3J(^1H, ^1H)$ = 8 Hz, 2H), 2.42 (s, 3H),

2.01 (s, 6H). ESI + MS: m/z = 773.098 $[M - Cl]^+$ (calc.: 773.1051), 1656.115 $[2M + K]^+$ (calc.: 1656.1019), 1657.115 $[2M + K]^+$ (calc.: 1657.1097).

***fac*-[Re(NPhF)Cl$_3$(PPh$_3$)(CNPh^{NO2})Cl$_3$] (6).** Recrystallization from CH_2Cl_2/toluene. Green, very unstable plates. Yield: 28 mg, 40%. The compound quickly decomposes in solution, which goes along with a color change to brown and precludes the measurement of the solution spectra of reasonable quality. IR (cm^{-1}): 2160 (s, $\nu_{N\equiv C}$), 1735 (m, $\nu_{N=O}$). ^{1}H NMR (acetone-d_6, ppm): δ = 8.32 (m_c, 2H), 7.79 (m_c, 6H), 7.42–7.32 (m, 9H), 7.12–7.05 (m, 4H), 6.88 (dd, $^3J(^1H, ^1H)$ = 8 Hz, 6H). ^{19}F NMR (acetone-d_6, ppm): δ = −100.4 (m_c). ESI + MS: m/z = 834.003 $[M + Na]^+$ (calc.: 834.003), 1647.013 $[2M + Na]^+$ (calc.: 1645.017).

***fac*-[Re(NPhF)Cl$_3$(PPh$_3$)(CNp-FAr^{DarF2})] (11).** Recrystallization from acetonitrile. Blue blocks. Yield: 82 mg, 67%. Elemental analysis: calc.: C: 46.7, H: 2.3, N: 2.3%. Found: C: 47.2, H: 2.3, N: 2.2%. IR (cm^{-1}): 2158 (s, $\nu_{N\equiv C}$). ^{1}H NMR (acetone-d_6, ppm): δ = 8.22 (s, 4H), 7.76 (s, 2H), 7.73 (d, $^3J(^1H, ^{19}F)$ = 8 Hz, 2H), 7.49 (m_c, 9H), 7.35 (m_c, 3H,), 7.22 (m_c, 6H), 6.75 (m_c, 2H), 6.62 (m_c, 2H). ^{19}F NMR (acetone-d_6, ppm): δ = −62.6 (s, 12F), −103.1 (m_c, 1F), −109.9 (t, $^3J(^{19}F,^1H)$ = 8 Hz, 1F). $^{13}C\{^1H\}$ NMR (acetone-d_6, ppm): δ = 163.42 (d, $^1J(^{13}C,^{19}F)$ = 260 Hz), 163.31 (d, $^1J(^{13}C,^{19}F)$ = 260 Hz), 150.41, 148.13, 139.71 (d, J = 10 Hz), 138.30, 135.12 (d, $J(^{13}C,^{31}P)$ = 10 Hz), 133.88 (d, $^1J(^{13}C,^{31}P)$ = 52 Hz), 132.46 (q, $^2J(^{13}C,^{19}F)$ = 33 Hz), 131.78, 131.14, 128.92 (d, $J(^{13}C,^{31}P)$ = 10 Hz), 128.62 (d, $^3J(^{13}C,^{19}F)$ = 10 Hz), 124.00 (q, $^1J(^{13}C,^{19}F)$ = 260 Hz), 123.77, 119.98, 119.04 (d, $^2J(^{13}C,^{19}F)$ = 26 Hz), 117.61 (d, $^2J(^{13}C,^{19}F)$ = 26 Hz). ESI + MS: m/z = 1231.015 $[M + Na]^+$ (calc.: 1231.020), 1246.989 $[M + K]^+$ (calc.: 1246.995), 2441.037 $[2M + Na]^+$ (calc.: 2441.043), 2457.010 $[2M + K]^+$ (calc.: 2457.017).

***fac*-[Re(NPhF)(PPh$_3$)Cl$_3$(CNPh^{pF})] (12).** Recrystallization from CH_2Cl_2/*n*-pentane. Green trapezoids. Yield: 60 mg, 76%. Elemental analysis: calc.: C: 47.4, H: 3.0, N: 3.6%. Found: C: 47.5, H: 3.1, N: 3.6%. IR (cm^{-1}): 2173 (vs, $\nu_{N\equiv C}$). ^{1}H NMR (CD_2Cl_2, ppm): δ = 7.80 (m_c, 6H), 7.39 (m_c, 9H), 7.18 (m_c, 2H), 7.08 (m_c, 2H), 7.03 (m_c, 2H), 6.85 (m_c, 2H). ^{19}F NMR (CD_2Cl_2, ppm): δ = −101.4 (m_c, 1F), −106.9 (m_c, 1F). $^{13}C\{^1H\}$ NMR (CD_2Cl_2, ppm): δ = 164.12 (d, ($^1J(^{13}C–^{19}F)$ = 260 Hz), 163.17 (d, ($^1J(^{13}C–^{19}F)$ = 260 Hz), 150.98, 140.81, 134.93 (d, $J(^{13}C–^{31}P)$ = 8 Hz), 133.16 (d, $^1J(^{13}C–^{31}P)$ = 54 Hz), 131.87, 129.49 (d, $^3J(^{13}C–^{19}F)$ = 10 Hz), 129.05 (d, $J(^{13}C–^{31}P)$ = 10 Hz), 127.65 (d, $^3J(^{13}C–^{19}F)$ = 10 Hz), 122.79, 117.70 (d, $^2J(^{13}C–^{19}F)$ = 25 Hz), 117.17 (d, $^2J(^{13}C–^{19}F)$ = 25 Hz). ESI + MS: m/z = 806.990 $[M + Na]^+$ (calc.: 807.008), 822.964 $[M + K]^+$ (calc.: 822.983), 1590.993 $[2M + Na]^+$ (calc.: 1591.028), 1607.002 $[2M + K]^+$ (calc.: 1606.966).

***fac*-[Re(NPhF)Cl$_3$(CNAr^{Mes2})$_2$] (7).** $[Re(NPhF)Cl_3(PPh_3)_2]$ (**1**) (92 mg, 0.1 mmol) was suspended in toluene (10 mL) and $CNAr^{Mes2}$ (68 mg, 0.2 mmol) was added to it. The mixture was heated under reflux and the progress of the reaction was monitored by ^{19}F NMR. The solution became blue and homogeneous upon heating. After three hours, the complete starting material was consumed. Volatiles were removed under reduced pressure and the resulting blue solid was resuspended in *n*-pentane, filtered and washed with more *n*-pentane. Blue needles suitable for X-ray diffraction were obtained by slow evaporation of the toluene solution at 5 °C. Yield: 18 mg, 17%. Elemental analysis: calc.: C: 62.2, H: 5.0, N: 3.9%. Found: C: 62.4, H: 5.1, N: 3.9%. IR (cm^{-1}): 2192 (s, $\nu_{C\equiv N}$), 2163 (s, $\nu_{C\equiv N}$). ^{1}H NMR (CD_2Cl_2, ppm): δ = 7.52 (dd, $^3J(^1H,^1H)$ = 8 Hz, 2H), 7.27 (d, $^3J(^1H,^1H)$ = 8 Hz, 4H), 7.85 (dd, $^3J(^1H,^1H)$ = 8 Hz, 2H), 6.83 (s, 4H), 6.74 (s, 4H), 6.43(m_c, 2H), 2.22 (s, 12H), 2.01 (s, 12H), 1.98 (s, 12H). ^{19}F NMR (CD_2Cl_2, ppm): δ = −101.1 (m_c). $^{13}C\{^1H\}$ NMR (CD_2Cl_2, ppm): δ = 163.39 (d, $^1J(^{13}C,^{19}F)$ = 260 Hz), 150.20 (br. S), 140.13, 138.08, 136.17 (d, $^3J(^{13}C,^{19}F)$ = 14 Hz), 135.21, 133.13, 131.61, 130.27, 128.89, 128.72, 128.58 (d, $^4J(^{13}C,^{19}F)$ = 9 Hz), 125.03, 117.14 (d, $^2J(^{13}C,^{19}F)$ = 24 Hz), 21.38, 20.69, 20.29. ESI + MS: m/z = 1044.3266 $[M - Cl]^+$ (calc.: 1044.3224), 1102.2871 $[M + Na]^+$ (calc.: 1102.2850), 2183.5903 $[2M + Na]^+$ (calc.: 2183.5718).

***mer*-[Re(NPhF)Cl$_3$(CNAr^{Dipp2})$_2$] (8).** $[Re(NPhF)Cl_3(PPh_3)_2]$ (**1**) (92 mg, 0.1 mmol) was suspended in toluene (4 mL) and $CNAr^{Dipp2}$ (128 mg, 0.3 mmol) was added to it. The mixture was heated under reflux and the progress of the reaction was monitored by ^{19}F NMR. After 4 h, the starting complex was completely consumed. The volatiles were removed under reduced pressure and the obtained blue solid was suspended in *n*-pentane, filtered off, and washed with further *n*-pentane. Blue single crystals suitable for X-ray diffraction were obtained from CH_2Cl_2/toluene. Yield: 46 mg, 37%. Elemental analysis: calc.: C: 65.4, H: 6.3, N: 3.4%. Found: C: 65.4, H: 6.1, N: 3.1%. IR (cm^{-1}): 2170 (vs, $\nu_{N\equiv C}$). ^{1}H NMR (CD_2Cl_2, ppm): δ = 7.47 (dd, $^3J(^1H,^1H)$ = 7 Hz), 7.28 (d, $^3J(^1H,^1H)$ = 8 Hz, 4H), 7.12 (dd, $^3J(^1H,^1H)$ = 8 Hz), 7.06 (m_c, 2H), 7.02–6.98 (m, 10H), 2.42 (hept, $^3J(^1H,^1H)$ = 7 Hz), 1.05 (d, $^3J(^1H,^1H)$ = 8 Hz, 24H), 1.03 (d, $^3J(^1H,^1H)$ = 8 Hz, 24H). ^{19}F NMR (CD_2Cl_2, ppm): δ = −103.4 (m_c). $^{13}C\{^1H\}$ NMR (CD_2Cl_2, ppm): δ = 160.43 (d, $^1J(^{13}C,^{19}F)$ = 260 Hz), 153.48, 146.77, 140.32, 133.35, 130.83, 130.17, 129.57, 125.34, 124.25 (d, $^3J(^{13}C,^{19}F)$ = 10 Hz), 123.17, 117.84 (d, $^2J(^{13}C,^{19}F)$ = 25 Hz), 31.54, 24.57, 24.13. ESI + MS: m/z = 1270.4715 $[M + Na]^+$ (calc.: 1270.46951).

***fac*-[Re(NPhF)Cl$_3$(PPh$_3$)(CNAr^{Tripp2})] (9).** $[Re(NPhF)Cl_3(PPh_3)_2]$ (**1**) (92 mg, 0.1 mmol) was suspended in toluene (6 mL) and $CNAr^{Tripp2}$ (102 mg, 0.2 mmol) dissolved in toluene (2 mL) was added to it. The mixture was heated under reflux and the progress of the reaction was monitored by ^{19}F NMR. After one hour, only the resonances of the starting material and one other compound were observed. The heating was stopped and a few blue needles suitable for X-ray diffraction were obtained by slow evaporation of the crude reaction mixture at 5 °C.

***mer*-[Re(NPhF)Cl$_3$(CNAr^{Tripp2})$_2$] (10).** $[Re(NPhF)Cl_3(PPh_3)_2]$ (**1**) (92 mg, 0.1 mmol) was suspended in toluene (6 mL) and $CNAr^{Tripp2}$ (102 mg, 0.2 mmol) dissolved in toluene (2 mL) was added to it. The mixture was heated under reflux and the progress of the reaction was monitored by ^{19}F NMR. After 12 h, complex **1** was nearly completely consumed. The volatiles were removed under reduced pressure and the residue was dissolved in diethyl ether and filtered. The solvent was removed under reduced pressure leading to a blue powder. Blue single crystals suitable for X-ray diffraction were obtained from diethyl ether/

n-hexane. Yield: 116 mg, 82%. Elemental analysis: calc.: C: 67.8, H: 7.3, N: 3.0%. Found: C: 67.9, H: 7.3, N: 3.0%. IR (cm^{-1}): 2170 (vs, $\nu_{N\equiv C}$). ^1H NMR (CD_2Cl_2, ppm): δ = 7.47 (dd, $^3J(^1H,^1H)$ = 8 Hz, 2H), 7.31 (d, $^3J(^1H,^1H)$ = 8 Hz, 4H), 7.07 (m_c, 2H), 6.93 (s, 8H), 6.86 (m_c, 2H), 2.82 (h, $^3J(^1H,^1H)$ = 7 Hz, 4H), 2.38 (h, $^3J(^1H,^1H)$ = 7 Hz, 8H), 1.28 (d, $^3J(^1H,^1H)$ = 8 Hz, 24H), 1.02 (d, $^3J(^1H,^1H)$ = 8 Hz, 24H), 0.95 (d, $^3J(^1H,^1H)$ = 8 Hz, 24H). ^{19}F NMR (CD_2Cl_2, ppm): δ = −104.1 (m_c). $^{13}C\{^1H\}$ NMR (CD_2Cl_2, ppm): δ = 160.43 (d, $^1J(^{13}C,^{19}F)$ = 260 Hz), 153.96, 149.74, 146.40, 141.49, 131.18, 130.76, 130.46, 126.09, 123.59 (d, $^3J(^{13}C,^{19}F)$ = 10 Hz), 121.75, 117.52 (d, $^2J(^{13}C,^{19}F)$ = 24 Hz), 34.99, 31.67, 24.91, 24.53, 24.09. ESI + MS: *m*/*z* = 1438.644 $[M + Na]^+$ (calc.: 1436.657), 1454.618 $[M + K]^+$ (calc.: 1454.631).

Conclusions

The results of the present study may demonstrate that the use of fluorine-substituted ligand systems can have a number of benefits apart from their use in pharmaceutical approaches, but also for fundamental chemical studies. (1) The introduction of the fluorine or CF_3 substituent modulates the solubility *e.g.* of the starting materials, (2) reactions with diamagnetic compounds can readily be monitored (and thus optimized) by means of ^{19}F NMR, (3) the use of a peripheral *m,m′*-$(CF_3)_2Ar$ group is a suitable instrument to control the steric bulk of ligand systems and (4) fluorine substituents are well suitable to control the electronic properties of ligand systems.

Author contributions

Conceptualization: U. A., J. S. F., and G. C.; methodology: M. R. J. and A. H; validation: G. C. and E. K.; formal analysis: G. C., E. K, A. H., and M. R. J.; investigation: G. C., E. K., and U. A.; resources: U. A.; writing – original draft preparation: U. A.; writing – review and editing: U. A., J. S. F., G. C., M. R. J., and E. K.; visualization: U. A. and G. C.; supervision: U. A., J. S. F., and G. C.; project administration: G. C. and U. A.; funding acquisition: U. A. and J. S. F. All authors have read and agreed to the published version of the manuscript.

Conflicts of interest

There are no conflicts to declare.

Acknowledgements

This research was funded by the DFG (Deutsche Forschungsgemeinschaft: Graduate School BIOQIC), the U.S. National Science Foundation (International Supplement to CHE-1802646), and the Alexander von Humboldt Foundation (fellowship to J. S. F.). We acknowledge the assistance of the Core Facility BioSupraMol supported by the DFG and of the High-Performance-Computing (HPC) Centre of the Zentraleinrichtung für Datenverarbeitung (ZEDAT) of the Freie Universität Berlin for computational time and support.

References

1 E. P. Gillis, K. J. Eastman, M. D. Hill, D. J. Donnelly and N. A. Meanwell, *J. Med Chem.*, 2015, **58**, 8315.
2 F. Salsi, G. Bulhões Portapilla, S. Simon, M. Roca Jungfer, A. Hagenbach, S. de Albuquerque and U. Abram, *Inorg. Chem.*, 2019, **58**, 10129.
3 Y. Zhou, J. Wang, Z. Gu, S. Wang, W. Zhu, J. Luis Aceña, V. A. Soloshonok, K. Izawa and H. Liu, *Chem. Rev.*, 2016, **116**, 422.
4 O. Jacobsen, D. O. Kiesewetter and X. Chen, *Bioconjugate Chem.*, 2015, **26**, 1–18.
5 R. Halder and T. Ritter, *J. Org. Chem.*, 2021, **86**, 13873–13884.
6 U. Abram, Innovative PET and SPECT tracers, in *Quantification of Biophysical Parameters in Medical Imaging*, ed. I. Sack and T. Schaeffter, Springer International, 2017, pp. 255–279.
7 M. D. Bartholomä, A. S. Louie, J. F. Valliant and J. Zubieta, *Chem. Rev.*, 2010, **110**, 2903.
8 C. S. Cutler, H. M. Hennkens, N. Sisay, S. Huclier-Markai and S. S. Jurisson, *Chem. Rev.*, 2013, **113**, 858.
9 F. Salsi, M. Roca Jungfer, A. Hagenbach and U. Abram, *Eur. J. Inorg. Chem.*, 2020, **13**, 1222.
10 G. Claude, J. Genz, D. Weh, M. Roca Jungfer, A. Hagenbach, M. Gembicky, J. S. Figueroa and U. Abram, *Inorg. Chem.*, 2022, **61**, 16163.
11 G. Claude, D. Weh, A. Hagenbach, J. S. Figueroa and U. Abram, *Z. Anorg. Allg. Chem.*, 2022, e202200320.
12 M. C. Gil Valenzuela, J. Környei, M. Mikolajzak, K. Ozker, M. R. A. Pillai, M. Venkatesh, E. B. Araujo, M. Dondi, S. C. Gomes, R. Koga, E. Lavie, Z. F. Luo, J. Mustansar, D. V. S. Narasimhan, W. Paragulla, A. Robles and S. Verdera, *Technetium-99m Radiopharmaceuticals: Manufacture* of Kits, IAEA Technical Reports Series No. 466, International Atomic Energy Agency, Vienna, Austria, 2008, pp. 126–129.
13 L. W. Herman, V. Sharma, J. F. Kronauge, E. Barbaric, L. Herman and D. Piwnica-Worms, *J. Med. Chem.*, 1995, **38**, 2955–2963.
14 D. Piwnica-Worms, J. F. Kronauge, B. L. Holman, A. Davison and A. G. Jones, *Invest. Radiol.*, 1989, **24**, 25–29.
15 J. F. Kronauge and D. J. Mindiola, *Organometallics*, 2016, **35**, 3432–3435.
16 F. E. Hahn, L. Imhof and T. Lügger, *Inorg. Chim. Acta*, 1998, **269**, 347–349.
17 J. Bryan, R. E. Stenkamp, T. H. Tulip and J. M. Mayer, *Inorg. Chem.*, 1987, **26**, 2283–2288.
18 J. S. Figueroa and U. Abram, *Z. Anorg. Allg. Chem.*, 2020, **646**, 909–914.
19 G. Claude, F. Salsi, A. Hagenbach, M. Gembicky, M. Neville, C. Chan, J. S. Figueroa and U. Abram, *Organometallics*, 2020, **39**, 2287–2294.

20 G. Claude, L. Zeh, M. Roca Jungfer, A. Hagenbach, J. S. Figueroa and U. Abram, *Molecules*, 2022, **27**, 8546.
21 U. Abram, Rhenium, in *Comprehensive Coordination Chemistry II*, ed. J. A. McCleverty and T. J. Meyer, Elsevier, 2003, vol. 5, pp. 271–403.
22 G. K. Lahiri, S. Goswami, L. R. Falvello and A. Chakravorty, *Inorg. Chem.*, 1987, **26**, 3365–3370.
23 C. M. Archer, J. R. Dilworth, P. Jobanputra, M. E. Harman, M. B. Hursthouse and A. Karaulov, *Polyhedron*, 1991, **10**, 1539–1543.
24 M. Bakir, S. Paulson, P. Goodson and B. P. Sullivan, *Inorg. Chem.*, 1992, **31**, 1127–1129.
25 Yu.-P. Wang, C.-M. Che, K.-Y. Wong and S.-M. Peng, *Inorg. Chem.*, 1993, **32**, 5827–2832.
26 M. A. Masood and D. J. Hodgson, *Inorg. Chem.*, 1994, **33**, 2488–2490.
27 M. A. Masood, B. P. Sullivan and D. J. Hodgson, *Inorg. Chem.*, 1994, **33**, 5360–5362.
28 H. Luo, I. Setyawati, S. J. Rettig and C. Orvig, *Inorg. Chem.*, 1995, **34**, 2287–2299.
29 M. Bakir and B. P. Sullivan, *J. Chem. Soc., Dalton Trans.*, 1995, 1733–1738.
30 M. T. Ahmet, B. Coutinho, J. R. Dilworth, J. R. Miller, S. J. Parrott, Y. Zheng, M. Harman, M. B. Hursthouse and A. Malik, *J. Chem. Soc., Dalton Trans.*, 1995, 3041–3048.
31 M. Bakir, J. A. M. McKenzie and B. P. Sullivan, *Inorg. Chim. Acta*, 1997, **254**, 9–17.
32 F. Refosco, C. Bolzati, F. Tisato and G. Bandoli, *J. Chem. Soc., Dalton Trans.*, 1998, 923–930.
33 M. A. Masood, B. P. Sullivan and D. J. Hodgson, *Inorg. Chem.*, 1999, **38**, 5425–5430.
34 A. L. Suing, C. R. Dewan, P. S. White and H. H. Thorp, *Inorg. Chem.*, 2000, **39**, 6080–6085.
35 X. Couillens, M. Gressier, R. Turpin, M. Dartiguenave, Y. Coulais and A. L. Beauchamp, *J. Chem. Soc., Dalton Trans.*, 2002, 914–924.
36 M. Porchia, F. Tisato, F. Refosco, C. Bolzati, M. Cavazza-Ceccato, G. Bandoli and A. Dolmella, *Inorg. Chem.*, 2005, **44**, 4766–4776.
37 H. Braband, D. Przyrembel and U. Abram, *Z. Anorg. Allg. Chem.*, 2006, **632**, 779–785.
38 B. Kuhn and U. Abram, *Z. Anorg. Allg. Chem.*, 2008, **634**, 2982–2988.
39 B. Kuhn and U. Abram, *Z. Anorg. Allg. Chem.*, 2011, **637**, 242–245.
40 H. H. Nguyen, C. T. Pham and U. Abram, *Polyhedron*, 2015, **99**, 216–222.
41 S. Majumder, J. P. Naskar, A. Bhattacharya, R. Ganguly, P. Saha and S. Chowdhury, *J. Coord. Chem.*, 2015, **68**, 599–615.
42 P. Saha, J. P. Naskar, A. Bhattacharya, R. Ganguly, B. Saha and S. Chowdhury, *J. Coord. Chem.*, 2016, **69**, 303–317.
43 M. Roca Jungfer, A. Hagenbach, E. Schulz Lang and U. Abram, *Eur. J. Inorg. Chem.*, 2019, 4974–4984.
44 A. P. Borges, B. Possato, A. Hagenbach, A. E. H. Machado, V. M. Deflon, U. Abram and P. I. S. Maia, *Inorg. Chim. Acta*, 2021, **516**, 120110.
45 N. H. Huy and U. Abram, *Z. Anorg. Allg. Chem.*, 2008, **634**, 1560–1564.
46 X. Schoultz, T. I. A. Gerber, E. Hosten, R. Betz, L. Rhyman and P. Ramasami, *Polyhedron*, 2015, **96**, 6–15.
47 A. Barandov and U. Abram, *Polyhedron*, 2009, **28**, 1155–1159.
48 L. Wei, J. Zubieta and J. W. Babich, *Inorg. Chem.*, 2004, **43**, 6445–6454.
49 T. I. A. Gerber, D. Luzipo and P. Mayer, *Inorg. Chim. Acta*, 2004, **357**, 429–435.
50 J. B. Arterburn, K. V. Rao, D. M. Goreham, M. V. Valenzuela, M. S. Holguin, K. A. Hall, K. C. Ott and J. C. Bryan, *Organometallics*, 2000, **19**, 1789–1795.
51 C. Scholtysik, M. Roca Jungfer, A. Hagenbach and U. Abram, *Z. Anorg. Allg. Chem.*, 2018, **644**, 1451.
52 C. Scholtysik, C. Njiki Noufele, A. Hagenbach and U. Abram, *Inorg. Chem.*, 2019, **58**, 5241.
53 G. Bandoli, T. I. A. Gerber, J. Perilis and J. G. H. du Preetz, *Inorg. Chim. Acta*, 1998, **278**, 96–100.
54 M. T. Ahmet, B. Coutinho, J. R. Dilworth, J. R. Miller, S. J. Parrott and Y. Zheng, *Polyhedron*, 1996, **15**, 2041–2050.
55 T. D. Lohrey, E. A. Cortes, J. I. Fostvedt, A. L. Oanta, A. Jain, R. G. Bergman and J. Arnold, *Inorg. Chem.*, 2020, **59**, 11096–11107.
56 P. Patil, M. Ahmadian-Moghaddam and A. Dömling, *Green Chem.*, 2020, **22**, 6902–6911.
57 L. A. Labios, M. D. Millard, A. L. Rheingold and J. S. Figueroa, *J. Am. Chem. Soc.*, 2009, **131**, 11318–11319.
58 T. B. Ditri, B. J. Fox, C. E. Moore, A. L. Rheingold and J. S. Figueroa, *Inorg. Chem.*, 2009, **48**, 8362–8375.
59 B. J. Fox, M. D. Millard, A. G. DiPasquale, A. L. Rheingold and J. S. Figueroa, *Angew. Chem., Int. Ed.*, 2009, **48**, 3473–3477.
60 B. J. Fox, Q. Y. Sun, A. G. DiPasquale, A. R. Fox, A. L. Rheingold and J. S. Figueroa, *Inorg. Chem.*, 2008, **47**, 9010–9020.
61 G. W. Margulieux, N. Weidemann, D. C. Lacy, C. E. Moore, A. L. Rheingold and J. S. Figueroa, *J. Am. Chem. Soc.*, 2010, **132**, 5033–5035.
62 M. A. Stewart, C. E. Moore, T. B. Ditri, L. A. Labios, A. L. Rheingold and J. S. Figueroa, *Chem. Commun.*, 2011, **47**, 406–408.
63 D. W. Agnew, C. E. Moore, A. L. Rheingold and J. S. Figueroa, *Organometallics*, 2017, **36**, 363–371.
64 C. C. Mokhtarzadeh, C. E. Moore, A. L. Rheingold and J. S. Figueroa, *J. Am. Chem. Soc.*, 2018, **140**, 8100–8104.
65 D. W. Agnew, C. E. Moore, A. L. Rheingold and J. S. Figueroa, *Angew. Chem., Int. Ed.*, 2015, **54**, 12673–12677.
66 A. E. Carpenter, C. C. Mokhtarzadeh, D. S. Ripatti, I. Havrylyuk, R. Kamezawa, C. E. Moore, A. L. Rheingold and J. S. Figueroa, *Inorg. Chem.*, 2015, **54**, 2936.
67 D. W. Agnew, M. D. Sampson, C. E. Moore, A. L. Rheingold, C. P. Kubiak and J. S. Figueroa, *Inorg. Chem.*, 2016, **55**, 12400–12408.

68 D. W. Agnew, C. E. Moore, A. L. Rheingold and J. S. Figueroa, *Dalton Trans.*, 2017, **46**, 6700–6707.
69 M. J. Drance, J. D. Sears, A. M. Mrse, C. E. Moore, A. L. Rheingold, M. L. Neidig and J. S. Figueroa, *Science*, 2019, **363**, 1203–1205.
70 F. Salsi, M. Neville, M. Drance, A. Hagenbach, C. Chan, J. S. Figueroa and U. Abram, *Chem. Commun.*, 2020, **56**, 7009–7013.
71 F. Salsi, M. Neville, M. Drance, A. Hagenbach, J. S. Figueroa and U. Abram, *Organometallics*, 2021, **40**, 1336–1343.
72 N. Weidemann, G. W. Margulieux, C. E. Moore, A. L. Rheingold and J. S. Figueroa, *Inorg. Chim. Acta*, 2010, **364**, 238–245.
73 T. B. Ditri, A. E. Carpenter, D. S. Ripatti, E. Moore, A. L. Rheingold and J. S. Figueroa, *Inorg. Chem.*, 2013, **52**, 132216–113229.
74 F. Salsi, S. Wang, C. Teutloff, M. Busse, M. L. Neville, A. Hagenbach, R. Bittl, J. S. Figueroa and U. Abram, *Angew. Chem., Int. Ed.*, 2023, DOI: **10.1002/anie.202300254**.
75 G. M. Sheldrick, *SADABS*, University of Göttingen, Germany, 1996.
76 P. Coppens., *The Evaluation of Absorption and Extinction in Single-Crystal Structure Analysis. Crystallographic Computing*, Copenhagen, Muksgaard, 1979.
77 G. M. Sheldrick, A short history of SHELX, *Acta Crystallogr.*, 2008, **64**, 112.
78 G. M. Sheldrick, Crystal structure refinement with SHELXL, *Acta Crystallogr.*, 2015, **71**, 3.
79 O. V. Dolomanov, L. J. Bourhis, R. J. Gildea, J. A. K. Howard and H. Puschmann, *J. Appl. Crystallogr.*, 2009, **42**, 339–341.
80 H. Putz and K. Brandenburg, *DIAMOND, Crystal and Molecular Structure Visualization Crystal Impact, version 4.6.5*, GbR, Bonn, Germany, 2021.